# Optimization of the Single-Phased White Phosphor of $Li_2SrSiO_4$: $Eu^{2+}$, $Ce^{3+}$ for Light-Emitting Diodes by Using the Combinatorial Approach Assisted with the Taguchi Method

Lei Chen,*[†,‖] Anqi Luo,[†] Yao Zhang,[†] Fayong Liu,[†] Yang Jiang,[†] Qingsheng Xu,[†] Xinhui Chen,[†] Qingzhuo Hu,[†] Shi-Fu Chen,*[‡] Kuo-Ju Chen,[§] and Hao-Chung Kuo[§]

[†]School of Materials Science and Engineering, Hefei University of Technology, Hefei 230009, China

[‡]Department of Chemistry, Huaibei Normal University, Huaibei 235000, China

[§]Department of Photonic & Institute of Electro-Optical Engineering, National Chiao Tung University, Hsinchu 30010, Taiwan

[‖]Semiconductor and Optoelectronic Technology Engineering Research Center of Anhui Province, Wuhu 241000, China

**S** *Supporting Information*

**ABSTRACT:** The best performance of the phosphor $Li_2SrSiO_4$: $Eu^{2+}$, $Ce^{3+}$ in terms of luminescence efficiency (LE), color rendering index (CRI) and color temperature (Tc) for light-emitting diode application was optimized with combinatorial approach. The combinatorial libraries were synthesized with solution-based method and the scale-up samples were synthesized with conventional solid-reaction method. Crystal structure was investigated by using the X-ray diffraction spectrometer. The emission spectra of each sample in combinatorial libraries were measured in situ by using a fiber optic spectrometer. Fluorescence spectrometers were used to record excitation and emission spectra of bulk samples. White light generation was tuned up by tailoring $Eu^{2+}$ and $Ce^{3+}$ concentrations in the single-phased host of $Li_2SrSiO_4$ under near-ultraviolet excitation, but it exhibited low efficiency of luminescence and poor color rendering index. The effects of each level of the $Eu^{2+}$ and $Ce^{3+}$ concentrations on LE, CRI, and Tc were evaluated with the Taguchi method. The optimum levels of the interaction pairs between $Eu^{2+}$ and $Ce^{3+}$ concentration on LE, CRI, and Tc were [2, 1] (0.006 M, 0.003 M), [1, 2] (0.003 M, 0.006 M), and [3, 1] (0.009 M, 0.00 3M), respectively. The thermal stability of luminescence, the external quantum efficiency (QE), luminance, chromaticity coordinates, correlated color temperature, color purity including the composition ratio of RGB in white light, and color rendering index of the white light emission of phosphor were evaluated comprehensively from a bulk sample.

**KEYWORDS:** white light-emitting diodes, luminescence, phosphor, $Li_2SrSiO_4$: $Eu^{2+}$, $Ce^{3+}$, combinatorial approach, the Taguchi method
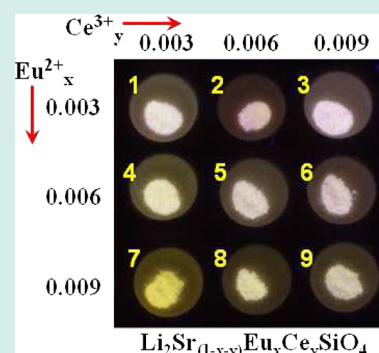
## 1. INTRODUCTION

White light-emitting-diodes (WLEDs) were considered as a new generation of green and energy-saving light source, owning small solid volume and strong ability to endure serious shock with high reliability.[1−4] For this reason, many efforts have been paid to replace the conventional compact fluorescent lamps with WLEDs.[5−8] Nevertheless, the white light was mainly produced by a combination of blue light from an InGaN LED chip and excited emission from the yellow phosphor of $Y_3Al_5O_{12}$:$Ce^{3+}$ (YAG) or by exciting three-primary phosphors with near-ultraviolet (NUV) emission of LEDs at present.[9,10] As for the YAG-based WLEDs, the blue emission of LED chips depends strongly on current strength, which will result in the luminescence color of WLEDs shift with current fluctuations, occasionally yellowish or partially bluish. As for the tricolor-phosphor-type WLEDs, the deposition, segregation, and inhomogeneous distribution of various phosphors because of their different particle sizes and densities will affect the luminescence color and efficiency of WLEDs.[11] In view of

these aspects, a single host activated with multiactivators which can emit white light was desired for WLEDs, especially those containing red composition with high CRI.[12,13]

The orange-yellow emission of $Li_2SrSiO_4$:$Eu^{2+}$ was first reported by Varadaraju,[14] and the improvement of red emission compared to the commercial YAG:Ce phosphor was obtained by coating the phosphor of $Li_2SrSiO_4$:$Eu^{2+}$ on an InGaN LED chip (max = 420 nm).[14] The yellow, yellow green, pure green and bluish green luminescence were observed in the ternary composition library of $Li_2SrSiO_4$:$Eu^{2+}$−$Li_2BaSiO_4$:$Eu^{2+}$−$Li_2CaSiO_4$:$Eu^{2+}$, including those unitary, binary, and mixtures, but in terms of both emission intensity and color chromaticity for WLEDs, the binary green phosphors with specific composition of $Li_2(Ba_{1−x}Sr_x)SiO_4$:$Eu^{2+}$ (0.28 < $x$ < 0.56) showed the best performance.[15] Moreover, the phosphor of

$Li_2SrSiO_4:Ce^{3+}$ displays blue emission.[16] Therefore, it is promising to produce white light by mixing the blue luminescence of $Ce^{3+}$ with the orange emission of $Eu^{2+}$.[14−17] Zou's[17] research work has suggested that $Li_2SrSiO_4:Eu^{2+}, Ce^{3+}$ could be a potential phosphor for WLED under NUV excitation and the intensity of luminescence maximized at $x = 0.075$ for $Li_2SrSiO_4:0.01Eu^{2+}·xCe^{3+}$. However, more details about the feasibility of the phosphor for LEDs application, such as, the relation about LE, CRI, Tc, chromaticity coordinates $CIE(x, y)$, and the concentrations of $Eu^{2+}$ and $Ce^{3+}$ with precise control levels, were not evaluated.

Combinatorial chemistry approach, which was initially developed to accelerate drug discovery, emerged as a technique for rapid synthesis and high-throughput screening of huge numbers of diverse compounds to search for new materials.[18−24] Nevertheless, even the largest combinatorial libraries that could be synthesized and screened only cover a small space of the well-known or unknown compounds.[25−30] To reduce the cost and time expended in the synthesis and characterization of innumerous compounds, some algorithms, including genetic, Monte Carlo techniques, simulated annealing guided evaluation, and artificial neural networks algorithms, have been adopted to compensate for the weakness of the combinatorial approach.[25−30] Undeniably, the application of algorithms in combinatorial approach has accelerated the discovery of new compounds, including biological targets, proteins, and nucleic acids.[25−30] As for inorganic phosphors, Sohn et al. employed the genetic algorithms, based on a global optimization strategy in which the evolutionary process is imitated with elitism, selection, crossover and random mutation operations, in the combinatorial approach to search for new luminescent materials for light-emitting diodes and plasma display panels.[31−33] The authors' previous research demonstrated that the performance of the combinatorial approach in evaluating the effects of components on an objective property, identifying the factors which one has the strongest effect and which one has minor effect, reducing the experimental dimensions of multifactors and estimating the expected performance under the optimal conditions, could be improved by combining with the Taguchi method.[34] Here, the method was further applied to optimize the white emission of $Li_2SrSiO_4:Eu^{2+}, Ce^{3+}$ phosphor for WLEDs.

## 2. EXPERIMENTAL PROCEDURES

The experimental design and data analysis carried out with the Taguchi method were proceeded automatically with the aid of a computer by using the software of Qualitek-4.[38] The combinatorial libraries were synthesized by inkjetting precursor solutions into array wells on an $Al_2O_3$ substrate in the sequence of $Sr \rightarrow Si \rightarrow Li \rightarrow Ce \rightarrow Eu$ for no less than three times, in a manner similar to that in refs 12 and 35. In our previous researchs, a reactor array containing about 11 × 11 wells with a diameter of 4 mm were used, but the experimental errors and consistency were hard to control for trace amounts of samples synthesized.[36,37] Here, the reactor array about 6 × 6 wells with a diameter of 8 mm was adopted. $Sr^{2+}$, $Ce^{3+}$, and $Eu^{3+}$ solutions were prepared by dissolving due amount of $LiNO_3$, $Sr(NO_3)_2$, $Ce(NO_3)_3$, and $Eu(NO_3)_3$ into deionized water, respectively; the silicon sol was prepared by hydrolyzing ethyl silicate tetraethyl orthosilicate (TEOS) in deionized water. 5% excess $Li^+$ was added to compensate its evaporation during high temperature sintering. After it was dried at 100−120 °C, the microreactors that contained the precursors were first presintered at 600 °C for 2 h in the air, and then cooled down to room temperature with the furnace. Next, the prefired samples were pulverized with a quartz pestle. Finally, the combinatorial libraries were sintered at 850 °C for 4 h in the reducing atmosphere of 10% $H_2$ + 90% $N_2$ to yield the desired samples. The pictures of the overall luminescence of samples in combinatorial libraries were taken by using a digital camera excited with a potable Hg lamp. The emission spectra of each sample in reactor array were collected in situ with a fiber optic spectrometer (Ocean Optics, Inc., USB4000-UV−vis-ES). By taking samples out from reactors, the excitation and emission spectra were measured with Hitachi F4500 spectrometer. Meanwhile, crystal structure was investigated by using X-ray diffraction (XRD) spectrometer (Rigaku, D/Max-rB) with Cu Ka radiation ($\lambda = 1.5418$ Å). Some scale-up samples were synthesized with the conventional solid state reaction method. The thermal stability of luminescence, relative luminance, the external quantum efficiency (QE), color chromaticity, Tc, CRI, color purity, and the ratio of RBG in white light of luminescence of bulk samples were characterized by using the EVERFINE EX-1000 spectrometer.

## 3. RESULT AND DISCUSSION

In case of not knowing about the ideal concentrations of $Eu^{2+}$ and $Ce^{3+}$ for producing white light, a combinatorial library with a larger concentration range of activators was synthesized first. Figure 1 presents composition maps and luminescence
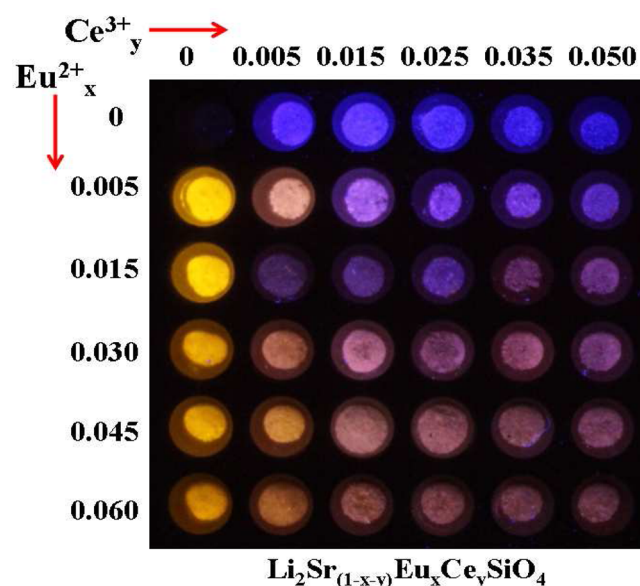


**Figure 1.** Composition map and luminescence photograph of the $Li_2(Sr_{1−x−y}Eu_xCe_y)SiO_4$ combinatorial library.

photograph of the $Li_2(Sr_{1−x−y}Eu_xCe_y)SiO_4$ combinatorial library under 365 nm excitation. As for the first sample in the top-left corner of the combinatorial library, no luminescence were observed from the host of $Li_2SrSiO_4$ for no $Eu^{2+}$ and $Ce^{3+}$ doping ($x = 0$ and $y = 0$). However, bright yellow luminescence is observed in the first longitudinal column with $x = 0.005−0.060$ and $y = 0$, and the luminance decreases with $Eu^{2+}$ increasing from $x = 0.005$ to $x = 0.060$ step by step. When the concentration of $Eu^{2+}$ is higher than 0.015 M, the luminescence decreases severely with its content increase. Similarly, bright blue emission was observed in the first

transverse column with $x = 0$ and $y = 0.005$–$0.050$. From the picture, it is difficult to discriminate the difference of luminance within the concentration range of $y = 0.005$, $0.015$, and $0.025$ M for $Ce^{3+}$, but the luminescence intensity decreases significantly when $Ce^{3+}$ concentration is higher than $0.025$ M. The emission spectra of each sample in the first longitudinal column and those in the first transverse column of combinatorial library were provided in Supporting Information Figures 1 and 2, respectively. A broad emission band with peaks at about 418 and 570 nm were observed, which were attributed to the $4f^05d^1 \rightarrow 4f^1$ transition of $Ce^{3+}$ and the $4f^65d^1 \rightarrow 4f^7$ transition of $Eu^{2+}$, respectively. Figure 2 presents the emission spectra of samples
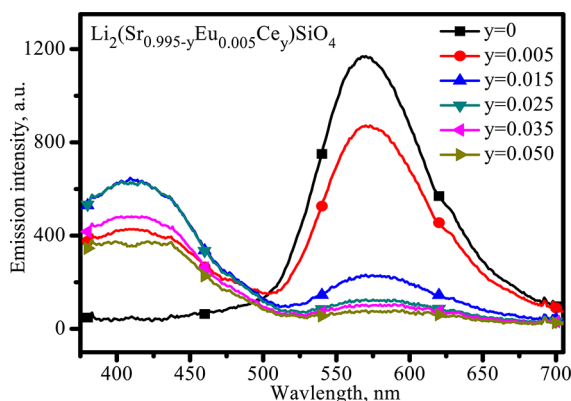


**Figure 2.** Emission spectra of $Li_2(Sr_{1-x-y}Eu_xCe_y)SiO_4$ ($x = 0.005$ and $y = 0$, $0.005$, $0.015$, $0.025$, $0.035$, and $0.050$), corresponding to the second transverse column samples in Figure 1.

in the second transverse column of the combinatorial library. The spectra consist of both $Eu^{2+}$ and $Ce^{3+}$ emissions. The luminescence intensity of $Ce^{3+}$ increases with its concentration initially from $y = 0$, maximizes at about $y = 0.005$–$0.015$ M, then decreases with $Ce^{3+}$ content increasing further, but the luminescence intensity of $Eu^{2+}$ decreases continuously with $Ce^{3+}$ concentration increasing from 0 to $0.050$ M. As revealed by the Supporting Information Figure 3, the overall luminescence intensity including both $Eu^{2+}$ and $Ce^{3+}$ emission achieved by integrating from 380 to 700 nm in Figure 2, increases as $Ce^{3+}$ concentration increases from $y = 0$, maximizes at $y = 0.005$, and then decreases seriously with the increase of $Ce^{3+}$ concentration,.

Figure 3 presents the XRD patterns of four samples of $Li_2(Sr_{1-x-y}Eu_xCe_y)SiO_4$ ($x = 0$, $y = 0$; $x = 0.06$, $y = 0$; $x = 0$, $y = 0.05$; and $x = 0.06$, $y = 0.05$) in the corner of combinatorial library in Figure 1. The four samples exhibit the same diffraction peaks, which can be indexed to the phase of $Li_2SrSiO_4$ (ICSD 16-7334), and no other phases including Eu, Ce, or other species were detected. Therefore, samples were well synthesized in this work and the activators of $Eu^{2+}$ and $Ce^{3+}$ ions have entered into the crystal lattice of $Li_2SrSiO_4$. $Li_2SrSiO_4$ crystallizes as a hexagonal structure with a space group of $P3_121$ and lattice constants of $a = 5.0228$ (0) Å, $c = 12.4552$ (1) Å, $c/a = 2.4797$, $V$ (cell volume) = $272.13$ (0) Å$^3$, and $z = 3$. Since the ionic radius of $Eu^{2+}$ (1.09) and $Ce^{3+}$ (1.03) are approximate to $Sr^{2+}$ (1.12) but much larger than those of $Li^+$ (0.68) and $Si^{4+}$ (0.42), $Eu^{2+}$, and $Ce^{3+}$ should preferably occupy the site of $Sr^{2+}$ in the crystal lattice of $Li_2SrSiO_4$. The framework of $Li_2SrSiO_4$ crystal structure is formed by connecting $SiO_4$ and $LiO_4$ tetrahedron with $Sr^{2+}$ ions, where two $SiO_4$ and $LiO_4$ tetrahedrons share a common oxygen atom.
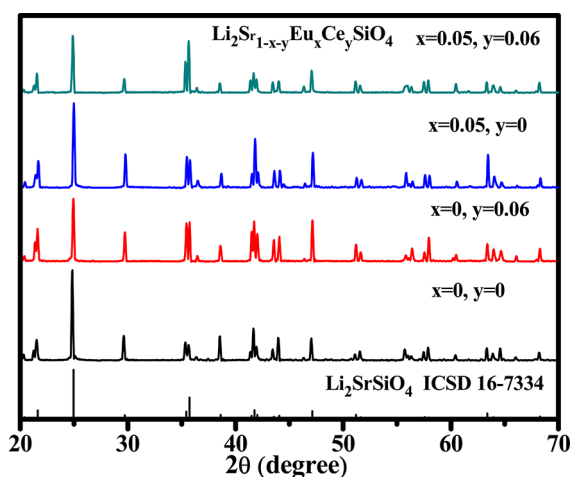


**Figure 3.** XRD patterns of $Li_2(Sr_{1-x-y}Eu_xCe_y)SiO_4$ ($x = 0$, $y = 0$; $x = 0.06$, $y = 0$; $x = 0$, $y = 0.05$; and $x = 0.06$, $y = 0.05$) compared with the standard ICSD 16-7334.

There is only one kind of site for $Sr^{2+}$ ions surrounded by 8 oxygen atoms. The three-dimensional crystal structure of $Li_2SrSiO_4$ which is drawn according to ICSD 16-7334 is displayed in Supporting Information Figure 4.

Figure 1 demonstrates that different emission color could be tuned up by changing $Eu^{2+}$ and $Ce^{3+}$ alternatively in $Li_2SrSiO_4$. However, the luminance seemingly decreases seriously with the increase of $Eu^{2+}$ and $Ce^{3+}$ contents, especially when the concentrations of $Eu^{2+}$ and $Ce^{3+}$ are higher than $0.015$ M. Thereby, it can be concluded that the reasonable concentration for both $Eu^{2+}$ and $Ce^{3+}$ to achieve efficient emission should not exceed $0.015$ M. To obtain highly efficient white light generation, thus, a second combinatorial library was synthesized.

The experimental design and analysis were dealt with the Taguchi method.[34] In this study, two factors each with three levels of concentration, which are 1 ($0.003$ M), 2 ($0.006$ M), and 3 ($0.009$ M) for both $Eu^{2+}$ and $Ce^{3+}$, were to be optimized. Therefore, the L-9 ($_3{}^4$) orthogonal array, which can accommodate four factors each with three levels, was selected to perform this experiment. The first and the second columns in the L-9 orthogonal array were set for the factors of $Eu^{2+}$ and $Ce^{3+}$, respectively, and the third and the fourth columns were used to accommodate the interaction between the first and the second columns. Table 1 gives the experimental design, in which the 9 trial conditions represent the composition of the 9 samples to be optimized. The 9 samples were collected in a combinatorial library, synthesized with the same method as above.

Figure 4a displays the composition map and luminescence picture of the combinatorial library. Intuitively, white luminescence was tuned up within the concentration range of $0.003$–$0.009$ M. Settled the concentration of $Ce^{3+}$ at $0.003$ M, the luminescence color of phosphors become yellowish as $Eu^{2+}$ concentration increases from $0.003$ through $0.006$ to $0.009$ M, seen from the first longitudinal column. Likewise, the emission color becomes bluish as $Ce^{3+}$ concentration increases from $0.003$ through $0.006$ to $0.009$ M when the concentration of $Eu^{2+}$ is fixed to $0.003$ M, displayed in the first traverse in Figure 4a. Figure 4b, c, and d presents the emission spectra of the 9 samples in the order of $Eu^{2+}$ concentration increase and fixed the concentration of $Ce^{3+}$ at $y = 0.003$, $0.006$, and $0.009$ for

**Table 1. Experimental Design and Results**

| | experimental design | | | | experimental results | | | | |
| | orthogonal array type L9($_3^4$) | | | | | | | | |
| columns | 1 | 2 | 3 | 4 | CIE | | | | |
| factors | $Eu^{2+}$ | $Ce^{3+}$ | inter cols 2 × 1 | inter cols 2 × 1 | $x$ | $y$ | Tc (K) | CRI (Ra) | external QE (%) |
| experiment 1 | 0.003 | 0.003 | Lev-1 | Lev-1 | 0.3924 | 0.3723 | 3648 | 62.7 | 24.459 |
| experiment 2 | 0.003 | 0.006 | Lev-2 | Lev-2 | 0.3459 | 0.2904 | 4613 | 69.4 | 24.187 |
| experiment 3 | 0.003 | 0.009 | Lev-3 | Lev-3 | 0.3578 | 0.3143 | 4243 | 67.1 | 27.539 |
| experiment 4 | 0.006 | 0.003 | Lev-2 | Lev-3 | 0.3716 | 0.3508 | 4058 | 64.9 | 31.46 |
| experiment 5 | 0.006 | 0.006 | Lev-3 | Lev-1 | 0.3738 | 0.351 | 3988 | 64.8 | 19.32 |
| experiment 6 | 0.006 | 0.009 | Lev-1 | Lev-2 | 0.3714 | 0.331 | 3881 | 64.5 | 20.5 |
| experiment 7 | 0.009 | 0.003 | Lev-3 | Lev-2 | 0.4377 | 0.4417 | 3272 | 57.9 | 17.441 |
| experiment 8 | 0.009 | 0.006 | Lev-1 | Lev-3 | 0.4013 | 0.3839 | 3533 | 60.4 | 18.889 |
| experiment 9 | 0.009 | 0.009 | Lev-2 | Lev-1 | 0.3845 | 0.363 | 3776 | 62.7 | 16.922 |
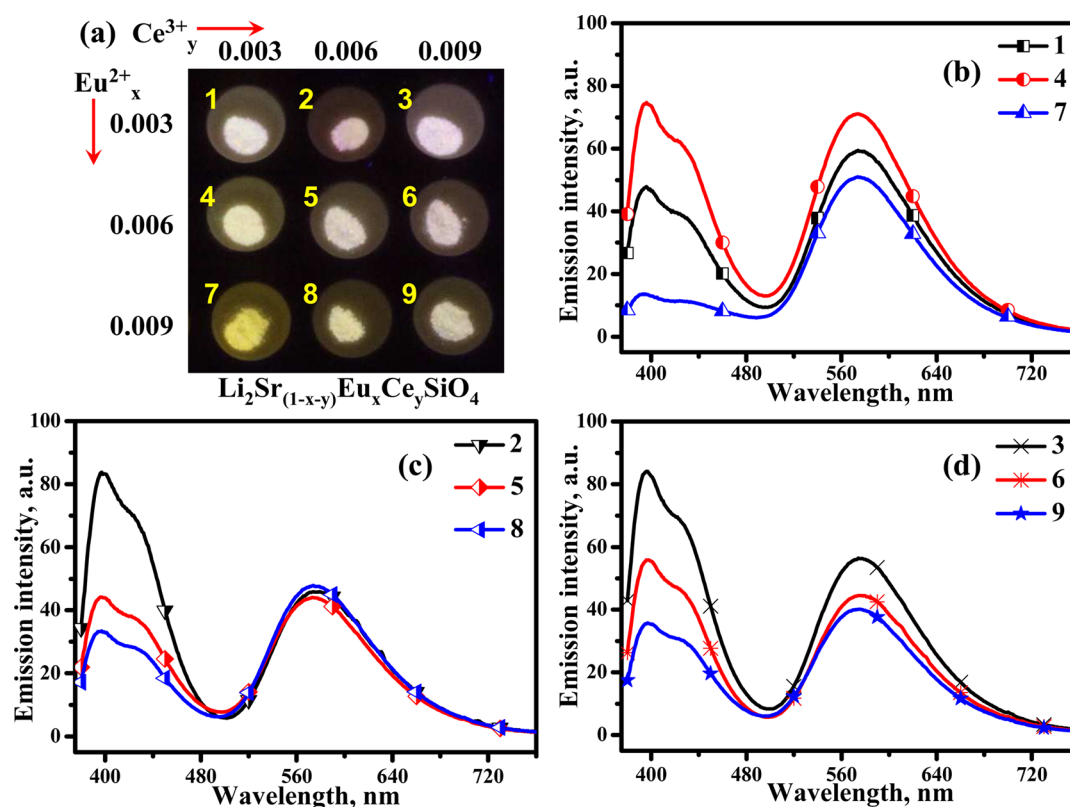


**Figure 4.** Composition map and luminescence photograph of combinatorial library and emission spectra of samples excited with 365 nm.

$Li_2(Sr_{1-x-y}Eu_xCe_y)SiO_4$, respectively. The chromaticity coordinates CIE($x$, $y$), CRI, Tc, and the external QE of the 9 samples were provided in Table 1. The external QE reaches its maximum at the experiment 4 condition as $x$ = 0.006 and $y$ = 0.003 for $Li_2(Sr_{1-x-y}Eu_xCe_y)SiO_4$ and the Tc about 4058 K at this condition is appropriate, but the CRI about 64.9 is very low. The lowest Tc about 3272 K occurs under the experiment 7 condition ($x$ = 0.009 for $Eu^{2+}$ and $y$ = 0.003 for $Ce^{3+}$), presenting warm white. The highest CRI about 69.4 occuring under the experiment 2 condition ($x$ = 0.003 for $Eu^{2+}$ and $y$ = 0.006 for $Ce^{3+}$) is far below than the ordinary value about Ra 85 or more for home-lighting. The CIE (0.3714, 0.3310) under the experiment 6 condition is nearest to the standard CIE (0.3333, 0.3333) coordinates of white light. In short, the parameters that reflect the quality of emission color on LE, CRI, Tc, and chromaticity cannot reach their best values at one condition for the same $Eu^{2+}$ and $Ce^{3+}$ concentrations.

Figure 5 presents the CIE coordinates of the emission spectra of samples 2, 5, and 8, showing that luminescence color shifts from pure white to yellow white step by step with $Eu^{2+}$ concentration increasing from $x$ = 0.003 through 0.006 to 0.009 M as $Ce^{3+}$ concentration is fixed on $y$ = 0.006 M. Although the Tc of the emission at the experiment 8 condition is very warm, its CRI still is very low. Obviously, the emission spectrum is short of red component, as demonstrated with color purity analysis in the later. Otherwise, the CIE coordinates would shift toward the point of the triangle of red area.

To identify which factor combined with which level of concentration of $Eu^{2+}$ and $Ce^{3+}$ are most desirable for objective properties, the standard analysis by using the average values was adopted to perform the data process.[34] The "bigger-the-better" quality characteristic (QC) was selected for the analyses of LE and CRI, while the "smaller-the-better" QC is selected for the analysis of Tc. Figure 6a, b, and c shows the average values of
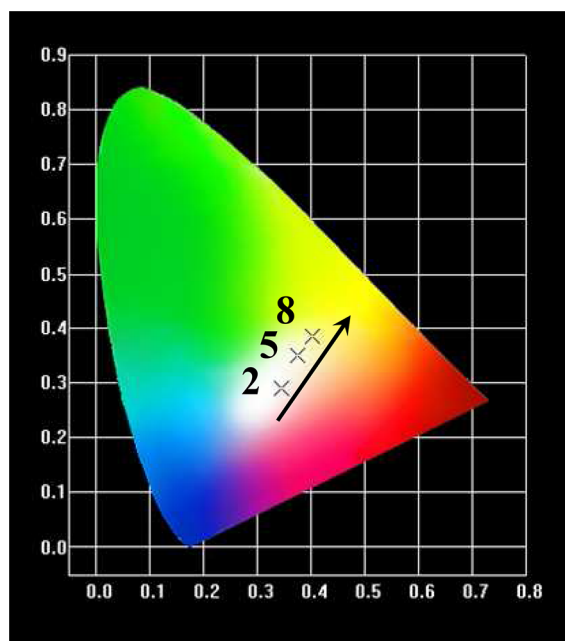
**Figure 5.** CIE coordinates of emission spectra of samples 2, 5, and 8.

each level of the control factors of $Eu^{2+}$ and $Ce^{3+}$ on the external QE, CRI, and Tc, respectively. The value of the external QE, CRI, and Tc vary significantly with $Eu^{2+}$ concentration, showing that $Eu^{2+}$ has great effect on them of all. Although the CRI and Tc change evidently with $Ce^{3+}$ concentration varying, the external QE does not alter significantly with the variation of $Ce^{3+}$ concentration, indicating that $Ce^{3+}$ has great effect on CRI and Tc but has little effect on LE. Thus, the statistical analysis of variance (ANOVA) was conducted to determine the significance of control factors on the LE, CRI, and Tc. Table 2 presents the results of ANOVA for each factor. The last column in the ANOVA table shows the relative effects of factors on the objective properties.[34] The sum of all percentage effects including experimental error totals to 100%. A high percentage effect means that the factor has great impact on objective property or the factor tolerance must be monitored carefully.[34] As revealed in Table 2, the relative effects of the factor $Eu^{2+}$ on the external QE, CRI, and Tc are about 49.64%, 62.88%, and 51.27%, respectively, while the effects of the factor $Ce^{3+}$ on the external QE, CRI and Tc are about 11.19%, 18.01%, and 19.67%. Considering the interaction between $Eu^{2+}$ and $Ce^{3+}$ as a third or a fourth factor, as shown in the last column in Table 2, they have great impact on the objective properties. For example, the influence of the factor 4 (i.e., the INTRE COLS 2*1) on the external QE for whose effect is about 30.96% is far higher than the effect about 11.94% of $Ce^{3+}$, which discloses an important mechanism of luminescence about the energy transfer from $Ce^{3+}$ to $Eu^{2+}$, as discussed in the following.

As far as the individual factor is concerned, the optimal level of concentration to achieve high LE, high CRI, and low Tc are 1 (0.003 M), 1 (0.003 M) and 3 (0.009 M) for the factor of $Eu^{2+}$, and 1 (0.003 M), 2 (0.006 M) and 1(0.003 M) or the factor $Ce^{3+}$, respectively. The contribution of factors at optimal condition to objective properties, the current grand average of performance, and the expected result at optimum conditions were disclosed in Supporting Information Table 1. However, the white light is produced by utilizing $Eu^{2+}$ and $Ce^{3+}$ emissions

together. Therefore, the interaction between $Eu^{2+}$ and $Ce^{3+}$ has to be considered as a factor. The optimum levels of the interaction pairs between $Eu^{2+}$ and $Ce^{3+}$ on the external QE, CRI, and Tc were [2, 1], [1, 2], and [3, 1], respectively, and the corresponding severity indexes (SI) were 40.81%, 38.59%, and 29.56%. More details about these results were shown in Supporting Information Table 2. In mathematics, the 100% of SI indicates the angle between two lines is 90 degrees, and the 0% of SI means the two lines are parallel with each other. Therefore, the value about 40.81% and 38.59% of SI on the external QE and CRI suggests that the interaction between $Eu^{2+}$ and $Ce^{3+}$ are crucial to the objective properties. Moreover, the low value about 29.56% of SI on Tc can account for why the Tc has been very warm but the CRI is very low, for deficiency of some conponents in the binary $Eu^{2+}$ and $Ce^{3+}$ emission spectrum.

The above combinatorial optimization demonstrates that the sample at the Experiment-7 condition can emit warm white light, but perform poor CRI and low LE. Herewith, a scale-up synthesis of this sample was conducted to compare this one with commercially available LED phosphors. Figure 7 presents the emission spectra of the bulk sample of $Li_2(Sr_{0.985}Eu_{0.006}Ce_{0.009})SiO_4$ excited with 365 nm at 30−150 °C. By normalizing the initial luminescence intensity to 100, the relative intensity of $Ce^{3+}$ emission at 412 nm and $Eu^{2+}$ emission at 570 nm as a function of temperature were displayed in Figure 8, which shows that the decrease of $Eu^{2+}$ emission upon temperature increasing is much more severe than that of $Ce^{3+}$, indicating that the thermal quench on $Eu^{2+}$ emission is more severe than on $Ce^{3+}$. The luminescence intensity integrated from 380 to 730 nm and the relative luminance of the phosphor, which comprises both $Ce^{3+}$ and $Eu^{2+}$ full-spectrum emission after considering the effect of visual sensitivity function were also displayed in Figure.8. The decrease of luminance with an increase of temperature is more rapidly than that of the integrated intensity of luminescence. This is because the green dominates the composition of the white light, revealed by color purity analysis as shown in Table 3. Table 3 summarizes the variation of luminance, the external QE, chromaticity coordinates CIE ($x$, $y$), Tc, CRI, color purity (%), and the ratio of RGB in the white light of emission of the phosphor upon temperature. The LE and Tc become worse but the CRI gets better with an increase of temperature. Besides the poor thermal stability of luminescence, the external QE about 27.54% at room temperature is lower than that of the commercial phosphors, such as, about 81% for the red phosphor of $CaAlSiN:Eu^{2+}$, 74% for the yellow phosphor of YAG, 66% for the green phosphor of $Lu_3Al_5O_{12}:Ce^{3+}$ (LuAG), and 44% for the blue phosphor of $BaMgAl_{10}O_{17}:Eu^{2+}$ (BAM). Additionally, Figure.7 discloses a significant difference between the mechanism of $Eu^{2+}$ and $Ce^{3+}$, where the emission spectra of $Ce^{3+}$ red shifts but $Eu^{2+}$ blue shifts with an increase of temperature. The red shift of emission spectrum usually is caused by the thermal vibration of electrons which intensifies with temperature increase. However, the blue shift of emission spectrum is caused by the phonon-coupling, in which the electrons are tuned from a low energy level to a higher one and then radiate light during electron transit from the high excited level to the ground state.

Finally, the excitation spectra were measured. The excitation spectra upon the emission of $Eu^{2+}$ at 570 nm and the emission of $Ce^{3+}$ at 418 nm of samples 2, 5, and 8 were displayed in Figure 9a and b, respectively. The wide band in the range of
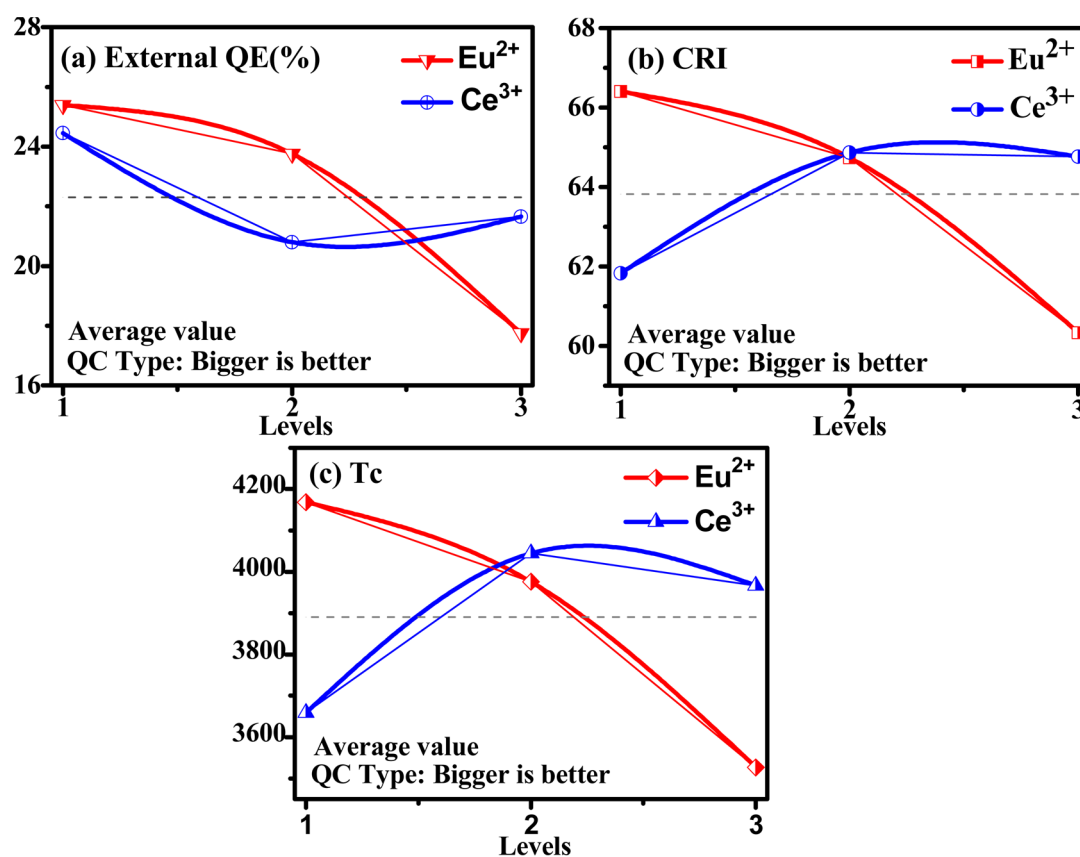
| | Factors | Level 1 | Level 2 | Level 3 |
|---|---|---|---|---|
| **External QE (%)** | 1 Factor A ($Eu^{2+}$) | 25.394 | 23.76 | 17.75 |
| | 2 Factor B ($Ce^{3+}$) | 24.453 | 20.798 | 21.653 |
| **CRI (Ra)** | 1 Factor A ($Eu^{2+}$) | 66.4 | 64.733 | 60.333 |
| | 2 Factor B ($Ce^{3+}$) | 61.833 | 64.866 | 64.766 |
| **Tc (k)** | 1 Factor A ($Eu^{2+}$) | 4168 | 3975.666 | 3527 |
| | 2 Factor B ($Ce^{3+}$) | 3659.333 | 4044.666 | 3966.666 |

**Figure 6.** Average values of each level of the factors of $Eu^{2+}$ and $Ce^{3+}$ on the properties of relative luminescence efficiency (LE), color rendering index (CRI), and color temperature (Tc).

**Table 2. Analysis of Variance (ANOVA) about the Significant Factors and Interaction Influences on Objective Properties**

| terms | column/factor | DOF ($f$) | sum of sqares ($S$) | variance ($V$) | pure sum ($s$) | percent $P$ (%) |
|---|---|---|---|---|---|---|
| external QE (%) | 1 factor $Eu^{2+}$ | 2 | 97.221 | 48.61 | 97.221 | 49.637 |
| | 2 factor $Ce^{3+}$ | 2 | 21.925 | 10.962 | 21.925 | 11.194 |
| | 3 inter cols 2 × 1 | 2 | 16.07 | 8.035 | 16.07 | 8.205 |
| | 4 inter cols 2 × 1 | 2 | 60.645 | 30.322 | 60.645 | 30.963 |
| CRI | 1 factor $Eu^{2+}$ | 2 | 58.942 | 29.471 | 58.942 | 62.881 |
| | 2 factor $Ce^{3+}$ | 2 | 17.816 | 8.908 | 17.816 | 18.006 |
| | 3 inter cols 2 × 1 | 2 | 16.113 | 8.056 | 16.113 | 17.189 |
| | 4 inter cols 2 × 1 | 2 | 0.858 | 0.429 | 0.858 | 0.915 |
| Tc | 1 factor $Eu^{2+}$ | 2 | 649176.83 | 324588.415 | 649176.83 | 51.27 |
| | 2 factor $Ce^{3+}$ | 2 | 249021.68 | 124510.84 | 249021.68 | 19.667 |
| | 3 inter cols 2 × 1 | 2 | 333756.549 | 166878.274 | 333756.549 | 26.359 |
| | 4 inter cols 2 × 1 | 2 | 34226.814 | 17113.407 | 34226.814 | 2.703 |

380−500 nm in Figure 9a was attributed to the f−d transition of $Eu^{2+}$; and the band in the range of 330−380 nm with a peak at 363 nm in Figure 9b was assigned to the f−d transition of $Ce^{3+}$. The presence of $Ce^{3+}$ absorption in the excitation spectra of $Eu^{2+}$ indicates that there is an energy transfer from $Ce^{3+}$ to $Eu^{2+}$. Moreover, the excitation band of $Eu^{2+}$ overlaps with the
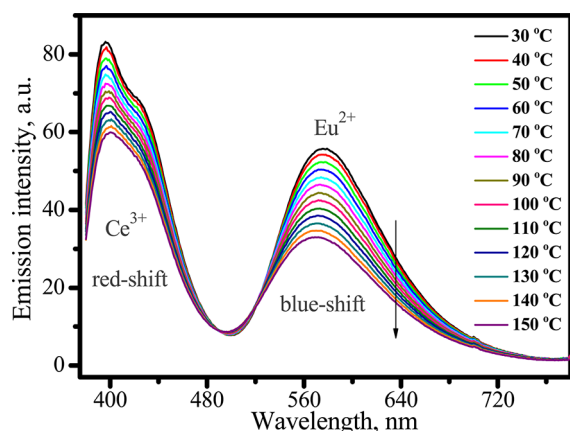
**Figure 7.** Emission spectra of $Li_2(Sr_{0.985}Eu_{0.006}Ce_{0.009})SiO_4$ excited with 365 nm at different temperature.
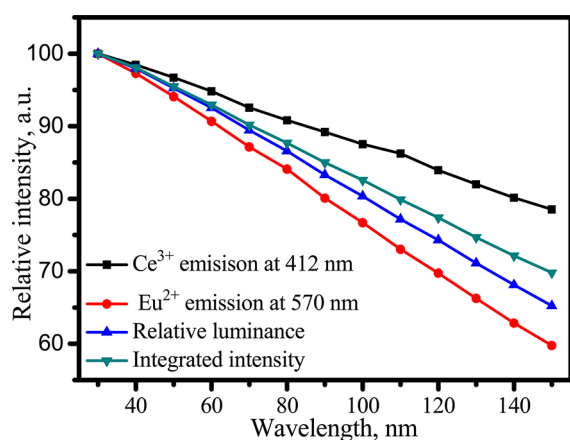


**Figure 8.** Normalized intensity of $Ce^{3+}$ emission at 412 nm and $Eu^{2+}$ emission at 570 nm and the overall luminescence intensity including both $Ce^{3+}$ and $Eu^{2+}$ integrated from 380 to 720 nm of $Li_2(Sr_{0.991}Eu_{0.006}Ce_{0.003})SiO_4$ as a function of temperature.

emission band of $Ce^{3+}$, as distinguished by comparing Figure 4 with Figure 9a. This point further demonstrates that there should exist in the energy transfer from $Ce^{3+}$ to $Eu^{2+}$. The

efficient energy transfer from $Ce^{3+}$ to $Eu^{2+}$ was observed in Fu's[40] experiment. However, the previous research reported by Kim pointed out that the energy transfer from $Ce^{3+}$ to $Eu^{2+}$ does not contribute to the enhancement of luminescence as for the $Eu^{2+}$ and $Ce^{3+}$ doubled-doped $Li_2SrSiO_4$ phosphor.[39]

If there were an efficient energy transfer from $Ce^{3+}$ to $Eu^{2+}$, the luminescence intensity of $Eu^{2+}$ should enhance correspondingly with $Ce^{3+}$ content increasing before reaching to its critical concentration; and the increase of $Eu^{2+}$ emission should at the expense of $Ce^{3+}$ emission accordingly. Settled $Ce^{3+}$ concentration at 0.003 M, Figure 4b shows that the luminescence of both $Eu^{2+}$ and $Ce^{3+}$ increases with $Eu^{2+}$ increasing from 0.003 to 0.006 M, indicating that the concentrations of $Eu^{2+}$ and $Ce^{3+}$ at 0.003 M are lower than their critical concentrations. Another reasonable explanation was that a little $Ce^{3+}$-ion doping could stabilize the vacancies caused by $Li^+$ evaporation and inhibits the oxidization of $Eu^{2+}$ to $Eu^{3+}$. Accordingly, the luminescence was improved.[39] When $Ce^{3+}$ concentration was fixed to 0.006 M, Figure 4c shows that the intensity of $Ce^{3+}$ decreases continuously with $Eu^{2+}$ concentration increasing from 0.003 through 0.006 to 0.009 M, suggesting that the energy was transferred from $Ce^{3+}$ to $Eu^{2+}$. But the luminescence of $Eu^{2+}$ does not increase accordingly, maybe because the content of $Eu^{2+}$ has reached to its critical concentration. To some extent, the energy could not be transferred from $Ce^{3+}$ to $Eu^{2+}$ efficiently. When the concentration of $Ce^{3+}$ was 0.009 M, both $Eu^{2+}$ and $Ce^{3+}$ luminescence decrease with $Eu^{2+}$ increasing from 0.003 to 0.009 M, because the concentrations of $Ce^{3+}-Eu^{2+}$ are higher than their critical concentrations. Here, we can conclude that there is some energy transfer from $Ce^{3+}$ to $Eu^{2+}$ but that this energy transfer is not very efficient. $Eu^{2+}$ and $Ce^{3+}$ compete with each other to snatch the excitation energy during luminescence in the system of $Eu^{2+}$- and $Ce^{3+}$-codoped $Li_2SrSiO_4$. $Eu^{2+}$ could emit by capturing excitation energy by itself, rather than depending on the energy transfer from $Ce^{3+}$ to $Eu^{2+}$.

## 4. CONCLUSIONS

In summary, white light generation from the single-phased $Li_2SrSiO_4$ system was tuned up tailoring $Eu^{2+}$ and $Ce^{3+}$ concentrations. As far as the biggest contribution of individual

**Table 3. Luminance, External Quantum Efficiency (QE), Chromaticity Coordinates (CIE ($x$, $y$)), Color Temperature (Tc), Color Purity, the Composition Ratio of RGB in White Light, and Color Rendering Index (CRI) of the Emission of the Phosphor $Li_2(Sr_{0.985}Eu_{0.006}Ce_{0.009})SiO_4$ as Function of Temperature**

| temp (°C) | lumin (cd/m²) | extern QE (%) | CIE | | Tc (K) | color purity (%) | red percent (%) | green percent (%) | blue percent (%) | CRI (Ra) |
| | | | $x$ | $y$ | | | | | | |
|---|---|---|---|---|---|---|---|---|---|---|
| 30 | 100 | 27.54 | 0.359 | 0.314 | 4188 | 7.8 | 18.6 | 78.6 | 2.9 | 66.8 |
| 40 | 97.98 | 27.00 | 0.3576 | 0.314 | 4248 | 7.6 | 18.4 | 78.7 | 2.9 | 67.1 |
| 50 | 95.26 | 26.26 | 0.3556 | 0.314 | 4336 | 7.2 | 18.2 | 78.9 | 2.9 | 67.5 |
| 60 | 92.53 | 25.55 | 0.3535 | 0.3137 | 4427 | 6.9 | 18 | 79 | 3 | 68 |
| 70 | 89.45 | 24.77 | 0.3514 | 0.3131 | 4523 | 8.1 | 17.8 | 79.1 | 3 | 68.5 |
| 80 | 86.60 | 24.07 | 0.3492 | 0.3122 | 4617 | 7.9 | 17.7 | 79.2 | 3.1 | 69 |
| 90 | 83.30 | 23.29 | 0.3465 | 0.3107 | 4739 | 7.9 | 17.5 | 79.3 | 3.2 | 69.7 |
| 100 | 80.36 | 22.59 | 0.3439 | 0.3094 | 4865 | 7.9 | 17.3 | 79.4 | 3.3 | 70.3 |
| 110 | 77.18 | 21.82 | 0.3409 | 0.3079 | 5013 | 8 | 17.1 | 79.5 | 3.3 | 70.8 |
| 120 | 74.28 | 21.10 | 0.338 | 0.3065 | 5166 | 8.2 | 16.9 | 79.7 | 3.4 | 71.5 |
| 130 | 71.11 | 20.33 | 0.3349 | 0.3047 | 5336 | 8.6 | 16.7 | 79.8 | 3.5 | 72.1 |
| 140 | 68.12 | 19.60 | 0.3318 | 0.3027 | 5521 | 8.4 | 16.5 | 79.9 | 3.6 | 72.7 |
| 150 | 65.25 | 18.92 | 0.3287 | 0.3004 | 5712 | 9.1 | 16.3 | 80 | 3.7 | 73.3 |
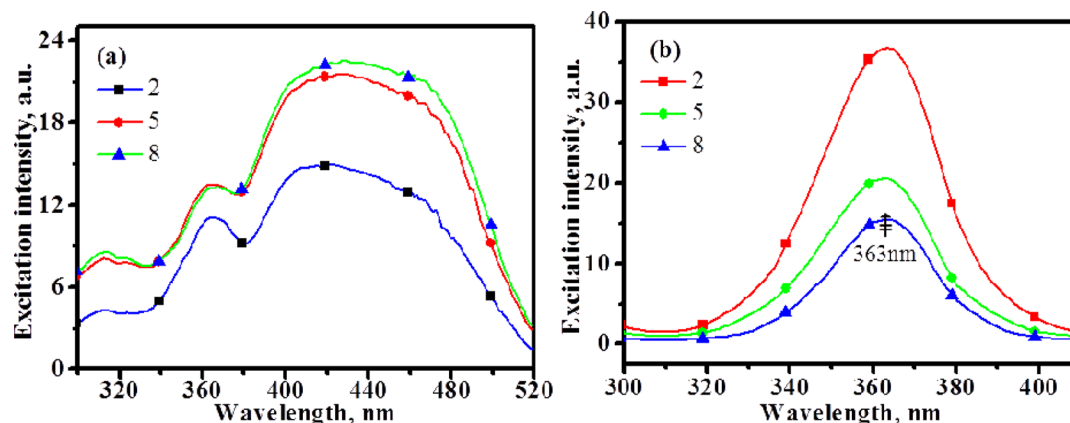
**Figure 9.** Excitation spectra of samples 2, 5, and 8.

factor on objective properties is concerned, the optimum concentration to achieve high luminescence efficiency, high color rendering index, and low correlated color temperature are 0.003 M, 0.003 M, and 0.009 M for the factor of $Eu^{2+}$ and 0.003 M, 0.006 M, and 0.003 M for the factor of $Ce^{3+}$, respectively respectively. The interaction pairs between $Eu^{2+}$ and $Ce^{3+}$ were processed as a factor to obtain the best performance in terms of high luminescence efficiency, high color rendering index, and low correlated color temperature: the optimum concentration is (0.006 M, 0.003 M), (0.003 M, 0.006), and (0.009 M, 0.003 M). The phosphor performs low thermal stability of luminescence and poor color rendering ability. The luminance of $Li_2(Sr_{0.985}Eu_{0.006}Ce_{0.009})SiO_4$. emission under 365 nm excitation losses about 35% with temperature increasing from 30 to 150 °C. The emission of $Ce^{3+}$ red shifts, while the emission of $Eu^{2+}$ blue shifts with an increase of temperature, which results in the color rendering ability get better with temperature increasing although the luminescence efficiency and correlated color temperature become worse. The analyses by using the Taguchi method reveals that $Eu^{2+}$ and $Ce^{3+}$ have different effects on the objective properties of luminescence efficiency, color rendering index, and color temperature, which provides an important clue to understand the mechanism of luminescence and accounts for why the parameters of the objective properties cannot maximize at the same one concentration of $Eu^{2+}$ and $Ce^{3+}$. The value of low severity index between $Eu^{2+}$ and $Ce^{3+}$ interaction on luminescence intensity indicates the energy could not transfer from $Ce^{3+}$ to $Eu^{2+}$ efficiently, where $Eu^{2+}$ and $Ce^{3+}$ compete with each other to snatch the excitation energy. $Eu^{2+}$ could emit by capturing excitation by itself, rather than depending on the energy transfer. The low severity index between $Eu^{2+}$ and $Ce^{3+}$ on the color rendering index suggests that the spectrum comprises of $Eu^{2+}$ and $Ce^{3+}$ emission was deficient in red and blue components, demonstrated with color purity calculation.

## ASSOCIATED CONTENT

### ⓢ Supporting Information

Emission spectra of some samples in combinatorial library, their integrated intensity of luminescence, the three-dimensional crystal structure, optimum conditions and performance of different factors, their interaction, and optimal levels achieved by calculating with the Taguchi method. This material is available free of charge via the Internet at http://pubs.acs.org.

## AUTHOR INFORMATION

### Corresponding Author

*E-mail: chichengfeiyang@yahoo.com.cn (L.C.); chshifu@ chnu.edu.cn (S.-F.C.). Phone: +86-551-2904566 (L.C.); +86-561-3606611 (S.-F.C.).

### Notes

The authors declare no competing financial interest.

## REFERENCES

(1) Schubert, E. F.; Kim, J. K. Solid-state light sources getting smart. *Science* **2005**, *308*, 1274−1278.

(2) Ye, S.; Xiao, F.; Pan, Y.; Ma, Y.; Zhang, Q. Phosphors in phosphor-converted white light-emitting diodes: Recent advances in materials, techniques and properties. *Mater. Sci. Eng., R* **2010**, *71*, 1−34.

(3) Xie, R.-J.; Hirosaki, N. Silicon-based oxynitride and nitride phosphors for white LEDs—A review. *Sci. Technol. Adv. Mater.* **2007**, *8*, 588−600.

(4) Chen, L.; Lin, C. C.; Yeh, C. W.; Liu, R. S. Light converting inorganic phosphors for white light-emitting diodes. *Materials* **2010**, *3*, 2172−2195.

(5) Jeong, H. H.; Lee, S. Y.; Choi, K. K.; Song, J. O.; Lee, J. H.; Seong, T. Y. Enhancement of light output power of GaN-based vertical light emitting diodes by optimizing *n*-GaN thickness. *Microelectron. Eng.* **2011**, *88*, 3164−3167.

(6) Zhmakin, A. I. Enhancement of light extraction from light emitting diodes. *Phys. Rep.* **2011**, *498*, 189−241.

(7) Pearsall, T.; Roussel, P.; Berlitz, S.; Heider, C.; Winkler, H.; Enderle, H.; Kuehn, C.; Petry, R.; Vosgroene, T.; Pohlmann, W. *Manuf. LEDs Light. Disp., Proc.* **2007**, *6797*, 0I−12.

(8) Yang, C. C.; Chang, C. L.; Huang, K. C.; Liao, T. S. The yellow ring measurement for the phosphor-converted white LED. *Phys. Proc.* **2011**, *19*, 182−187.

(9) Nakamura, S.; Fasol, G. *The Blue Laser Diode: GaN Based Blue Light Emitters and Lasers*; Springer, Berlin: 1997,pp 216.

(10) Sheu, J. K.; Chang, S. J.; Kuo, C.; Su, Y. K.; Wu, L.; Lin, Y.; Lai, W.; Tsai, J.; Chi, G. C.; Wu, R. White-light emission from near UV InGaN−GaN LED chip precoated with blue/green/red phosphors. *IEEE Photonics Technol. Lett.* **2003**, *15*, 18−20.

(11) Chen, L.; Chu, C. I.; Liu, R. S. Improvement of emission efficiency and color rendering of high-power LED by controlling size of phosphor particles and utilization of different phosphors. *Microelectron. Reliab.* **2011**, *52*, 900−904.

(12) Chen, L.; Chen, K. J.; Hu, S. F.; Liu, R. S. Combinatorial chemistry approach to searching phosphors for white light-emitting diodes in (Gd-Y-Bi-Eu) VO4 quaternary system. *J. Mater. Chem.* **2011**, *21*, 3677−3685.

(13) Huang, C. H.; Chen, T. M. A novel single-composition trichromatic white-light $Ca_3Y(GaO)_3(BO_3)_4:Ce^{3+}$, $Mn^{2+}$, $Tb^{3+}$ phosphor for UV-light emitting diodes. *J. Phys. Chem. C* **2011**, *115*, 2349−2355.

(14) Saradhi, M. P.; Varadaraju, U. Photoluminescence studies on $Eu^{2+}$-activated $Li_2SrSiO_4$: A potential orange-yellow phosphor for solid-state lighting. *Chem. Mater.* **2006**, *18*, 5267−5272.

(15) Kulshreshtha, C.; Sharma, A. K.; Sohn, K.-S. Effect of local structures on the luminescence of $Li_2(Sr,Ca,Ba)SiO_4:Eu^2$. *J. Electrochem. Soc.* **2009**, *156*, J52.

(16) Dotsenko, V. P.; Levshov, S. M.; Berezovskaya, I. V.; Stryganyuk, G. B.; Voloshinovskii, A. S.; Efryushina, N. P. Luminescent properties of $Eu^{2+}$ and $Ce^{3+}$ ions in strontium litho-silicate $Li_2SrSiO_4$. *J. Lumin.* **2011**, *131*, 310−315.

(17) Zhang, X.; He, H.; Li, Z.; Yu, T.; Zou, Z. Photoluminescence studies on $Eu^{2+}$ and $Ce^{3+}$-doped $Li_2SrSiO_4$. *J. Lumin.* **2008**, *128*, 1876−1879.

(18) Xiang, X. D.; Sun, X.; Briceno, G.; Lou, Y.; Wang, K. A.; Chang, H.; Wallace-Freedman, W. G.; Chen, S. W.; Schultz, P. G. A combinatorial approach to materials discovery. *Science* **1995**, *268*, 1738−1740.

(19) Briceno, G.; Chang, H.; Sun, X.; Schultz, P. G.; Xiang, X. D. A class of cobalt oxide magnetoresistance materials discovered with combinatorial synthesis. *Science* **1995**, *270*, 273−275.

(20) Janda, K. D.; Lo, L. C.; Lo, C. H. L.; Sim, M. M.; Wang, R.; Wong, C. H.; Lerner, R. A. Chemical selection for catalysis in combinatorial antibody libraries. *Science* **1997**, *275*, 945−948.

(21) Reddington, E.; Sapienza, A.; Gurau, B.; Viswanathan, R.; Sarangapani, S.; Smotkin, E. S.; Mallouk, T. E. Combinatorial electrochemistry: A highly parallel, optical screening method for discovery of better electrocatalysts. *Science* **1998**, *280*, 1735−1737.

(22) Danielson, E.; Golden, J. H.; McFarland, E. W.; Reaves, C. M.; Weinberg, W. H.; Di Wu, X. A combinatorial approach to the discovery and optimization of luminescent materials. *Nature* **1997**, *389*, 944−948.

(23) Wang, J.; Yoo, Y.; Gao, C.; Takeuchi, I.; Sun, X.; Chang, H.; Xiang, X. D.; Schultz, P. G. Identification of a blue photoluminescent composite material from a combinatorial library. *Science* **1998**, *279*, 1712−1714.

(24) Danielson, E.; Devenney, M.; Giaquinta, D. M.; Golden, J. H.; Haushalter, R. C.; McFarland, E. W.; Poojary, D. M.; Reaves, C. M.; Weinberg, W. H.; Di Wu, X. A rare-earth phosphor containing one-dimensional chains identified through combinatorial methods. *Science* **1998**, *279*, 837−839.

(25) Olender, R.; Rosenfeld, R. A fast algorithm for searching for molecules containing a pharmacophore in very large virtual combinatorial libraries. *J. Chem. Inf. Comput. Sci.* **2001**, *41*, 731−738.

(26) Gillet, V. J.; Khatib, W.; Willett, P.; Fleming, P. J.; Green, D. V. S. Combinatorial library design using a multiobjective genetic algorithm. *J. Chem. Inf. Comput. Sci.* **2002**, *42*, 375−385.

(27) Young, S. S.; Wang, M.; Gu, F. Design of diverse and focused combinatorial libraries using an alternating algorithm. *J. Chem. Inf. Comput. Sci.* **2003**, *43*, 1916−1921.

(28) Reynolds, C. H.; Tropsha, A.; Pfahler, L. B.; Druker, R.; Chakravorty, S.; Ethiraj, G.; Zheng, W. Diversity and coverage of structural sublibraries selected using the SAGE and SCA algorithms. *J. Chem. Inf. Comput. Sci.* **2001**, *41*, 1470−1477.

(29) Weber, L. Applications of genetic algorithms in molecular diversity. *Curr. Opin. Chem. Biol.* **1998**, *2*, 381−385.

(30) Schneider, G.; Wrede, P. Artificial neural networks for computer-based molecular design. *Prog. Biophys. Mol. Biol.* **1998**, *70*, 175−222.

(31) Sohn, K. S.; Park, D. H.; Cho, S. H.; Kim, B. I.; Woo, S. I. Genetic algorithm-assisted combinatorial search for a new green phosphor for use in tricolor white LEDs. *J. Comb. Chem.* **2006**, *8*, 44−49.

(32) Sohn, K. S.; Park, D. H.; Cho, S. H.; Kwak, J. S.; Kim, J. S. Computational evolutionary optimization of red phosphor for use in tricolor white LEDs. *Chem. Mater.* **2006**, *18*, 1768−1772.

(33) Jung, Y. S.; Kulshreshtha, C.; Kim, J. S.; Shin, N.; Sohn, K. S. Genetic algorithm-assisted combinatorial search for new blue phosphors in a $(Ca, Sr, Ba, Mg, Eu)_x B_y P_z O_\delta$ System. *Chem. Mater.* **2007**, *19*, 5309−5318.

(34) Chen, L.; Chu, C. I.; Chen, K. J.; Chen, P. Y.; Hu, S. F.; Liu, R. S. An intelligent approach to the discovery of luminescent materials using a combinatorial approach combined with Taguchi methodology. *J. Lumin.* **2011**, *26*, 229−238.

(35) Chen, L.; Chen, K. J.; Lin, C. C.; Chu, C. I.; Hu, S. F.; Lee, M. H.; Liu, R. S. Combinatorial approach to the development of a single mass $YVO_4$: $Bi^{3+}$, $Eu^{3+}$ phosphor with red and green dual colors for high color rendering white light-emitting diodes. *J. Comb. Chem.* **2010**, *12*, 587−594.

(36) Chen, L.; Bao, J.; Gao, C.; Huang, S.; Liu, C.; Liu, W. Combinatorial synthesis of insoluble oxide library from ultrafine/nano particle suspension using a drop-on-demand inkjet delivery system. *J. Comb. Chem.* **2004**, *6*, 699−702.

(37) Chen, L.; Fu, Y.; Zhang, G.; Bao, J.; Gao, C. Optimization of $Pr^{3+}$, $Tb^{3+}$, and $Sm^{3+}$ Co-doped $(Y_{0.65}Gd_{0.35}) BO_3$: $Eu_{0.05}^{3+}$ VUV phosphors through combinatorial approach. *J. Comb. Chem.* **2008**, *10*, 401−404.

(38) Roy, R. *Qualitek-4. Software for Automatic Design and Analysis of Taguchi Experiments*; Nutek, Inc.: Bloomfield Hills, MI, U.S.A., 2007.

(39) Kim, T.-G.; Lee, H.-S.; Lin, C. C.; Kim, T.; Liu, R.-S.; Chan, T.-S.; Im, S.-J. Effects of additional $Ce^{3+}$-doping on the luminescence of $Li_2SrSiO_4:Eu^{2+}$ yellow phosphor. *Appl. Phys. Lett.* **2010**, *96*, 061904−3.

(40) He, H.; Fu, R. L.; Cao, Y. G.; Song, X. F.; Pan, Z. W.; Zhao, X. R.; Xiao, Q. B.; Li, R. $Ce^{3+} \rightarrow Eu^{2+}$ energy transfer mechanism in the $Li_2SrSiO_4:Eu^{2+}$, $Ce^{3+}$ phosphor. *Opt. Mater.* **2010**, *32*, 632−636.